

DOI: 10.1002/marc.((insert number)) ((or ppap., mabi., macp., mame., mren., mats.))

## Feature Article

# **Taming macromolecules with light – Lessons learned from vibrational spectroscopy**

Jaana Vapaavuori,\* C. Geraldine Bazuin, Christian Pellerin\*

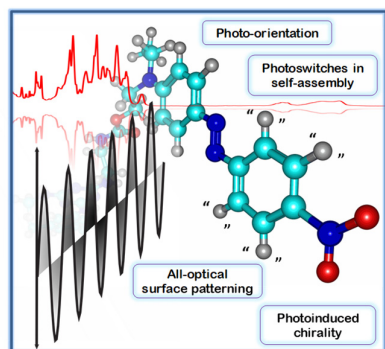
---

Dr. Jaana Vapaavuori, Prof. C. Geraldine Bazuin, Prof. Christian Pellerin  
Département de chimie, Université de Montréal, Montréal, QC, H3C 3J7, Canada  
E-mail: jaana.vapaavuori@umontreal.ca; c.pellerin@umontreal.ca

---

Exciting new applications, from large-area nanopatterning and templating to soft light-powered robotics, are emerging from the fundamental research on light-triggered changes in macromolecular systems upon photoisomerization of azobenzene-based molecular photoswitches. The understanding of how the initial molecular-scale photoisomerization of azobenzene, a complex photochemical event in itself, is translated into the response of macromolecules and even into macroscopic-scale motion of illuminated azomaterials is an enormous task. This feature article focuses on how this knowledge has advanced by applying different vibrational spectroscopy techniques that provide rich molecular insight into the photoresponse of chemically specific molecular moieties. In particular, we highlight infrared and Raman spectroscopic studies in the context of phototriggered perturbation of self-assembled structures, photoinduced linear and circular anisotropy, as well as photoinduced surface patterning, with the objective of offering a perspective on how vibrational spectroscopy can help in answering an array of essential yet unsettled questions.

FIGURE FOR ToC\_ABSTRACT



## 1. Introduction

Light is a powerful and tunable remote-control tool for photoresponsive macromolecules. The motivations for incorporating molecular photoswitches or light-powered motors within macromolecules can be roughly divided into two main categories. The first encompasses materials science and engineering purposes, such as designing new photoresponsive liquid crystals (LC), light-shaped micro- and nanofabrication templates, and photomechanical polymers for direct conversion of the electromagnetic energy of light into kinetic energy.<sup>[1-3]</sup> The second involves biological purposes, as in the external control of the structure and/or function of biomacromolecules such as peptides, proteins, nucleic acids, lipids, and carbohydrates.<sup>[4, 5]</sup> The term “photoswitching” can refer to many kinds of photoinduced chemical changes, such as the photolysis of covalent bonds,<sup>[6]</sup> photoinduced electron transfer<sup>[7]</sup> and ring-closure reactions,<sup>[8, 9]</sup> examples that highlight the diversity of photoswitching reactions.<sup>[10]</sup> For greater detail, reviews on the application of vibrational spectroscopy to rotaxane-based molecular machines,<sup>[11]</sup> molecular motors,<sup>[12]</sup> and molecule-based electronics, such as molecular electronic switches,<sup>[13]</sup> are highly recommended.

In this feature article, we will focus on one of the most commonly used photoswitches, both for materials engineering and biological applications, namely azobenzene.<sup>[14]</sup> This motif is known to change its geometry upon illumination with ultraviolet or visible light, in a so-called photoisomerization reaction from the thermodynamically stable trans conformation to the bent cis conformation (Figure 1a).<sup>[15, 16]</sup> This reaction can be used to both decrease and destroy existing order in materials, as in the cases of photoinduced unfolding of azobenzene-crosslinked alpha-helical peptides,<sup>[17]</sup> photoinduced nematic-isotropic phase transitions<sup>[18]</sup> and isothermal solid-to-liquid transitions,<sup>[19]</sup> or, on the contrary, to induce order and anisotropy in initially isotropic or less ordered materials, such as in photoinduced birefringence, photoinduced chirality, all-optical poling, and surface relief grating (SRG) formation.<sup>[2, 20, 21]</sup>

The photoisomerization of individual azobenzene moieties is known to occur in the picosecond timescale and results in changes in its molecular dimensions and properties, such as its dipole moment, solubility and UV-visible absorption.<sup>[15]</sup> Apolar azobenzene molecules typically have well isolated cis and trans absorption bands along with long thermal cis lifetimes. They are therefore suitable for optical switching applications where two "stable" long-lived states are required. In contrast, functionalizing azobenzene molecules with electron donating and electron withdrawing substituents (or push-pull substitution) alters their photochemistry, typically leading to an overlap of cis and trans absorption bands and thus to quasi-continuous photoswitching between the trans and cis geometrical isomers.<sup>[15, 16]</sup>

Examples of drastic changes in material systems resulting from bistable photoswitching between trans and long-lived cis isomers are illustrated in Figure 1b-d and include photoswitching of the tilt of liquid crystals by an azopolymer command layer,<sup>[22]</sup> the light-powered contraction of a helical ribbon of a liquid crystalline azopolymer, mimicking plant tendrils,<sup>[23]</sup> and the photoinduced decrease in helix content of a peptide cross-linked by an azobenzene.<sup>[17]</sup> Demonstrations of the use of continuous azobenzene photoswitching between the two geometrical isomers, shown in Figure 1e-g, include light-powered cantilever oscillators made of an azobenzene-containing liquid crystalline polymer<sup>[24, 25]</sup> and photoinduced surface patterning of azomaterials under polarization and/or intensity interference pattern irradiation, applicable as large-area micro- and nanofabrication templates,<sup>[26]</sup> as well as distributed feedback lasers.<sup>[27, 28]</sup> Despite such wide application prospects, a fundamental understanding of how the photoswitching of azobenzene is converted into a photoresponse of a macromolecular system is still incomplete although essential for optimizing these photoresponsive materials.

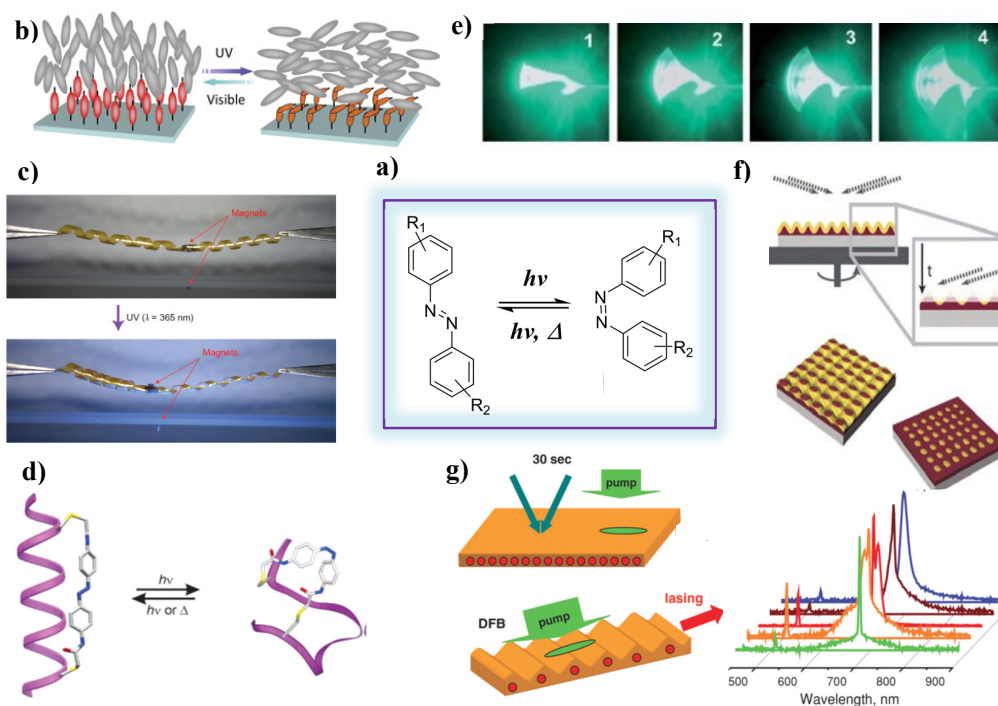


*Figure 1.* Azobenzene photoisomerization reaction (a, center) along with selected applications of azobenzene-containing macromolecular systems involving bistable (b-d, left side) and continuous (e-g, right side) photoswitching. b) Reversible photoalignment of liquid crystals by an azobenzene-containing command layer. c) Plant dendril mimicking light-powered ribbons that can move a magnet upon contraction of the ribbon. d) Light-induced unfolding of the helical structure of a peptide. e) Light-powered high-frequency cantilever oscillator. Photoinduced surface patterning of azopolymers f) employed as a template for the fabrication of plasmonic large-area gold nanohole arrays, and g) used as a building block for distributed feedback lasers. Figure 1b adapted with permission from Seki.<sup>[3]</sup> Copyright 2014. Nature Publishing Group. Figure 1c adapted with permission from Iamsaard et al.<sup>[23]</sup> Copyright 2014. Nature Publishing Group. Figure 1d adapted with permission from Woolley.<sup>[17]</sup> Copyright 2005. American Chemical Society. Figure 1e adapted with permission from Serak et al.<sup>[24]</sup> Copyright 2009. Royal Society of Chemistry. Figure 1f adapted with permission from Moerland et al.<sup>[26]</sup> Copyright 2014. Royal Society of Chemistry. Figure 1g adapted with permission from Goldenberg et al.<sup>[27]</sup> Copyright 2012. Wiley-VCH.

Many characterization methods can and should be combined to bridge the gap of understanding between photoinduced molecular processes and the photoresponse of macromolecular systems.

Vibrational spectroscopy can contribute to this goal since it provides a wealth of information about the molecular environment, including conformation, intra- and intermolecular interactions, and phase behavior (such as the presence of and dynamic changes in crystallinity or liquid crystalline mesophases).<sup>[29, 30]</sup> Linear infrared (IR) and Raman techniques are readily accessible and can often be coupled with illumination sources for in situ studies of the azomaterial photoresponse. IR and Raman spectroscopies are also powerful reporters of photoinduced orientation and (supra)molecular chirality when using linearly and circularly polarized light, respectively. This stems from their intrinsic chemical specificity that allows the contributions of specific moieties and individual components in complex systems to be distinguished, in contrast with classical techniques such as photoinduced birefringence and electronic circular dichroism. When comparing the two techniques, Raman spectroscopy has been less used to date than IR spectroscopy for resolving linear or circular anisotropy due to Raman spectroscopy's lower time resolution and higher complexity. With Raman spectroscopy, one must also ensure that the laser light is not in resonance with the azobenzene absorption or that the laser intensity is extremely low to avoid fluorescence and perturbation of the system (such as the introduction of photo-orientation by a linearly polarized probe beam).

Another capability of vibrational spectroscopy is that chemical information can be obtained with 2D or even 3D spatial resolution.<sup>[31-34]</sup> According to the Rayleigh criterion, the attainable resolution is given by  $0.61 \lambda / NA$ , where  $\lambda$  is the wavelength of light and NA is the numerical aperture of the objective. The spatial resolution in IR spectroscopy is restricted by long wavelengths (from  $\sim 3$  to  $20 \mu\text{m}$ ) while better resolution can be reached by Raman spectroscopy because a UV, visible or near-IR laser is employed (with  $\lambda_{\text{laser}}$  most commonly between 488 and 785 nm). Diffraction limited in-plane resolution can be reached for ideal samples such as individual carbon nanotubes for Raman spectroscopy and resolution targets for IR spectroscopy when using a focal plane array imaging system. In practice, a lower resolution on the order of  $10 \mu\text{m}$  for IR microscopy and 500 nm for confocal Raman microscopy is typically achieved for

thicker samples.<sup>[33]</sup> In Raman microscopy, better spatial resolution can be obtained by replacing the standard metallurgical objective by an immersion objective with a higher NA. For IR spectroscopy, the high refractive index of germanium allows an increase in NA by a factor of 4 for attenuated total reflection (ATR) imaging compared to transmission measurements and thus a corresponding resolution improvement.<sup>[32]</sup> It was recently shown that spatial oversampling with a pixel size on the order  $0.25 \lambda / \text{NA}$  provides the highest image quality and information content in the so-called hi-definition imaging mode.<sup>[35, 36]</sup> The depth resolution of confocal Raman microscopy is lower than its lateral resolution and is on the order of  $1 \mu\text{m}$  for ultrathin samples such as a suspended graphene sheet. In practice, the depth of focus degrades rapidly to several  $\mu\text{m}$  when probing below the surface of the sample and the focal volume is deeper than assumed due to refraction of light within the sample.<sup>[37, 38]</sup> These distortions can be alleviated by using an immersion objective. These various considerations are important to take into account in applications of spatially resolved vibrational spectroscopy to azopolymers.

Surface sensitivity down to a single monolayer or less can also be obtained using ATR or reflection-absorption IR spectroscopy<sup>[39]</sup> or surface-enhanced Raman scattering (SERS),<sup>[40]</sup> while more advanced techniques such as vibrational sum frequency generation can provide information about molecular organization and anisotropy specifically at the surface or at the buried interface between two bulk phases.<sup>[41]</sup> The time resolution of conventional IR and Raman spectroscopy is typically limited to several ms, which is sufficient for most studies at the material scale but is insufficient to probe the molecular details of the photoisomerization process itself. Specialized techniques, such as femtosecond stimulated Raman spectroscopy and ultrafast pump-probe spectroscopy, can shed light on the complexity of the many possible pathways of the azobenzene isomerization reaction and its impact on the structure and environment of surrounding molecules or molecular segments.<sup>[42]</sup>

Herein, we highlight four different application areas of macromolecular azo photoswitches where vibrational spectroscopy has advanced and continues to advance the molecular-level

understanding of photoresponsive materials. While examples of the applications of some of the most advanced techniques will be given, this feature will focus mainly on the approaches more readily accessible to polymer and materials scientists studying azo-based photoactive materials. The topics are organized in order of increasing light-induced order in the material. In section 2, non-polarized visible light is employed for disrupting order in the system, in particular to unfold peptides and to deform or rupture vesicles. Section 3 is devoted to the characterization of photoinduced uniaxial or biaxial anisotropy using linearly polarized IR and Raman. Section 4 explores how circularly polarized light can be used to create chiral structures and how these structures are studied by vibrational optical activity. Finally, in section 5, we describe the multiscale problem involving the characterization of surface patterns created by photoinduced mass transport of material under non-uniform illumination, such as polarization or intensity interference patterns. Even though the scope of this feature article is restricted to azobenzene-based photoresponsive macromolecular materials, we emphasize that vibrational techniques are broadly applicable to other types of photoswitches and to stimuli-responsive materials controlled by other external triggers besides light, such as pH, temperature, humidity and CO<sub>2</sub>.

## **2. Light control of self-assembled structures**

Many macromolecules, both of biological and synthetic origin, have the intrinsic characteristic of forming secondary or higher order structures based on folding due to specific intra- and intermolecular interactions. One way to build a fundamental understanding of the folding of biologically relevant proteins and of their synthetic polymer analogues is to study the stimulus-activated (un)folding dynamics of model peptides by either temperature (so-called T-jump experiments) or another external trigger, such as a photoswitch,<sup>[43]</sup> to induce structural changes at a scale much larger than the sub-nm scale of photoisomerization.<sup>[4,5]</sup> Although many different kinds of photoswitches have been covalently incorporated into model peptides, azobenzene derivatives were shown to give the largest range of activation wavelengths and cis lifetimes,



making them the most common photoswitch in foldamers; they can be incorporated in the foldamer backbone, tethered as a side chain or attached by both ends to create a loop connecting two parts of the foldamer.<sup>[44]</sup> All of these foldamer designs have been shown to lead to photoinduced changes, such as the helix-coil transition or photomodulation of the helicity.<sup>[45]</sup> One of the most accessible ways to determine the secondary structure of a peptide, and thus to observe its folding/unfolding, is to use IR to track the position of the amide I band (mainly due to C=O stretching of the peptide bond), which is very sensitive to intra- and intermolecular dipole-dipole coupling and hydrogen bonding.<sup>[46]</sup> It was shown by ultrafast UV pump/IR probe spectroscopy that the equilibration of the folded/unfolded peptide structures after a phototrigger event follows nontrivial dynamics with time constants distinct from the dynamics of the actual photoswitching reaction.<sup>[47-49]</sup>

Figure 2a illustrates the conclusions reached from applying a transient UV-visible pump to activate an azobenzene photoswitch located in the backbone of a  $\beta$ -hairpin structure via flexible linkers and using mid-IR and UV-visible probe spectroscopy to follow the structural changes in the  $\beta$ -hairpin upon photoinduced folding and unfolding.<sup>[50]</sup> The folding and unfolding, initiated by trans-cis and cis-trans azo isomerization, respectively, were found to follow the (fast) photoisomerization in a sequence of spectrally distinct steps, but with significant time differences. For unfolding, depicted in Figure 2a (right panel), stretching of the linkers with vibrational excess energy (represented by springs) as well as breakage of some intrastrand hydrogen bonds were observed at the scale of a few ps. However, the dense packing of the  $\beta$ -hairpin was still observed at the 25 ps scale and imposes constraints on the trans azobenzene and its adjacent linkers. The final unfolding took place at an order of magnitude slower time scale, being completed within 1 ns. In contrast, the fast trans-cis isomerization, depicted in the left panel of Figure 2a, also causes an initial local strain on the flexible linkers, but it is released much more quickly, with a 50 ps time constant, as compared to cis-trans isomerization. On the

other hand, the subsequent structural folding with intramolecular H-bond formation required a much longer thermal structural rearrangement, with a time constant in the  $\mu\text{s}$  range.<sup>[50]</sup>

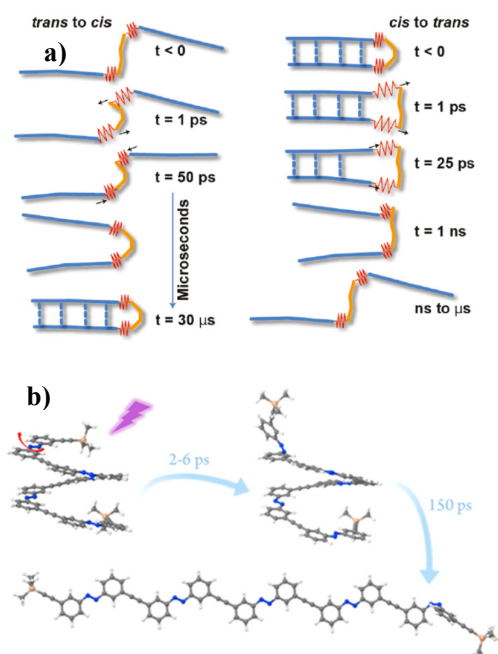


*Figure 2.* a) Stepwise structural changes related to the folding (photoinduced by the trans-to-cis reaction of the azobenzene photoswitch (left), depicted in orange), and the unfolding (photoinduced by the cis-to-trans reaction (right)) of a  $\beta$ -hairpin peptide, and the corresponding timescales determined by transient pump-probe spectroscopy. The orange springs represent the strain imposed on the flexible linkers by the (fast) photoisomerization reactions, leading to the (slower) peptide folding/unfolding and H-bond formation/breakage in the sequences shown. Reprinted with permission from Schrader et al.<sup>[50]</sup> Copyright 2011. American Chemical Society. b) Scheme of structural rearrangements occurring upon trans-to-cis photoisomerization in the backbone of a helical foldamer, leading to unfolding of the helical structure in acetonitrile at two distinct time scales. Reprinted with permission from Steinwand et al.<sup>[51]</sup> Copyright 2016. American Chemical Society.

UV pump (365 nm) / IR probe spectroscopy (5.6 to 8.5  $\mu\text{m}$ ) was also used to probe the mechanistic pathway of the first steps of photoinduced unfolding of a helical pentameric foldamer containing azobenzenes in the backbone, the changes in the vibrations of the side chain serving as fingerprints for unfolding.<sup>[51]</sup> The two observed timescales (20 and 150 ps)

were assigned to the completion of the initial photoisomerization event and the slower structural rearrangement steps of the foldamer structure (schematically illustrated in Figure 2b), respectively, and an unfolding reaction pathway supported by DFT calculations was proposed.<sup>[51]</sup> Direct structural resolution of these transient events could be significantly improved by applying transient 2D-IR spectroscopy, as reviewed by Hamm and co-workers.<sup>[52]</sup> A rather different application of light-control of self-assembled structures, having both biological and pharmaceutical application potential, centers on photoresponsive vesicles. In these spherical shell structures, water containing a useful cargo is enclosed by a membrane of amphiphilic small molecules (such as in liposomes) or block copolymers (polymersomes).<sup>[53]</sup> Combining optical laser trapping (optical tweezers) and the spatial resolution of confocal Raman spectromicroscopy allows collecting data from individual identifiable micrometer-sized vesicles. Under 365 nm UV illumination, bursting of the vesicles formed by a block copolymer of thermoresponsive N-isopropylacrylamide (NIPAM) and photoresponsive azo-containing repeat units (structure shown in Figure 3) was observed. Raman was used to determine in situ the degree of isomerization of the azobenzene with 1 s time resolution by following the appearance of cis-specific bands.<sup>[54]</sup> Cross-linking the azobenzene side groups in the otherwise same copolymer results in photoinduced swelling of the structure rather than bursting, and an increased degree of cross-linking leads to a decrease in both photoinduced swelling and degree of photoisomerization, as indicated in Figure 3.<sup>[55]</sup> It was also found that the swelling of the vesicles only occurs when azobenzene units are separated from the polymer backbone by a flexible spacer, whereas practically no photo-isomerization was observed in the absence of a spacer.<sup>[56]</sup> Optical laser trapping combined with Raman spectroscopy is an attractive method for investigating various types of self-assembled structures, not limited to macromolecules, that could offer interesting insights, for instance, on photoinduced release from liposomes.<sup>[57]</sup>

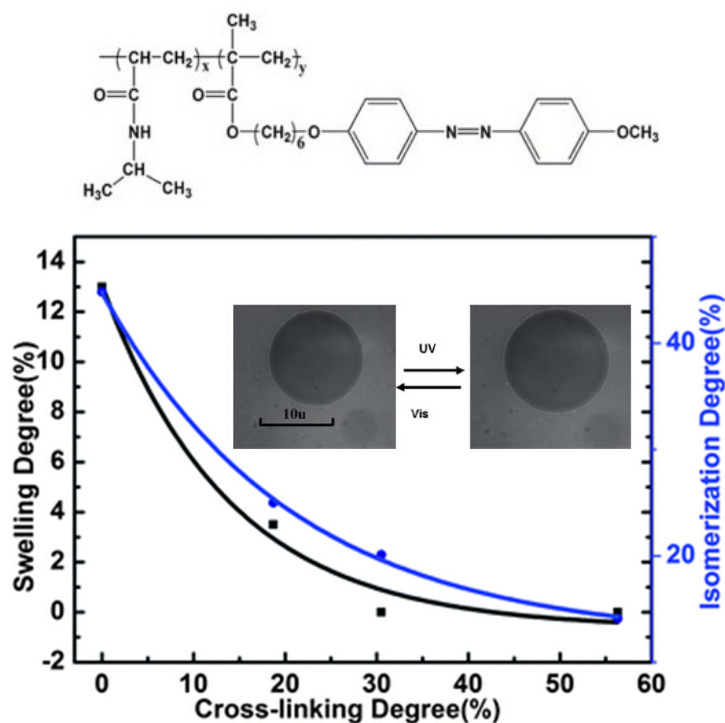
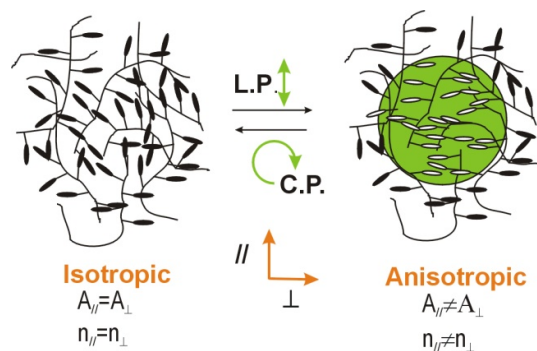


Figure 3. Photoinduced swelling and degree of azobenzene isomerization under 365 nm illumination as a function of cross-linking density in vesicles formed by the thermo- and photo-responsive diblock copolymer shown (before cross-linking). Reproduced with permission from Shen et al.<sup>[55]</sup> Copyright 2012. Royal Society of Chemistry.

### 3. Photo-orientation of azobenzenes and photocontrol of passive molecules

Photoinduced orientation of azobenzenes and of associated polymer chains and/or liquid crystalline domains can be achieved by illuminating azobenzene-containing macromolecules with linearly polarized light.<sup>[2]</sup> There are three main mechanisms affecting the induced orientation. First, angularly selective photoisomerization leads to an angle-dependent distribution of trans and cis isomers, so-called angular hole burning (AHB), because the probability of photon absorption by the trans azobenzene is proportional (with a  $\cos^2\theta$  dependence) to the projection of its transition dipole moment onto the electric field polarization direction of the incident radiation.<sup>[58]</sup> AHB is often followed by angular redistribution upon the cis-trans reaction and multiple trans-cis-trans isomerization cycles thus contribute to creating uniaxial photoinduced orientation perpendicular to the incident polarization direction, as

illustrated in Figure 4. Simultaneously, a relaxation process due to Brownian motion, also known as rotational diffusion, counteracts the angular redistribution of the molecules.<sup>[58, 59]</sup> This relaxation process also operates after the irradiation is removed and leads to partial loss of photoinduced orientation. The in-plane photoinduced orientation can be erased in many materials by further illumination with circularly polarized (Figure 4) or unpolarized light or by heating above the glass transition temperature. Multiple inscription and erasure steps can therefore be combined, although erasure with light leaves out-of-plane anisotropy in the material.<sup>[58]</sup> Photo-orientation of azobenzenes has interesting application prospects, such as all-optical inscription of waveguides,<sup>[60, 61]</sup> photoalignment of nanostructures in organic/inorganic hybrid films,<sup>[62]</sup> and command surfaces/layers, a concept widely applied for controlling the orientation of liquid crystals.<sup>[63]</sup>



*Figure 4.* Photo-orientation of an azobenzene-containing polymer by linearly polarized light and erasure of the induced orientation by circularly polarized light. Used with permission of François Lagugné-Labarthe.

Polarized IR spectroscopy has proven powerful for establishing a fundamental understanding of photo-orientation in macromolecules, since it elegantly complements polarized UV-visible spectroscopy and photoinduced birefringence studies by distinguishing the orientation and kinetics of specific chemical groups in the system. Buffeteau and Pérolet were the first to apply polarization modulation infrared linear dichroism (PM-IRLD) spectroscopy, coupled in situ

with a linearly polarized laser, to study the molecular-level photo-orientation of poly(Disperse Red 1 acrylate) (pDR1a), a well-characterized amorphous photoactive homopolymer.<sup>[64]</sup> PM-IRLD enables quantifying anisotropy in real time (down to a time resolution of 200 ms) by taking advantage of high-frequency photoelastic modulation between the two in-plane polarization directions. They observed that the orientation of several chemical groups assigned to azobenzene occurs simultaneously with the lower orientation of the carbonyl group near the main chain of pDR1a upon irradiation, and thus concluded that the short ethylene spacer of pDR1a allows partial translation of the orientation of the azo group into orientation of the main chain.<sup>[64, 65]</sup> In a library of closely related methacrylate-based polymers with longer alkyl spacers (4 to 12 methylene units), only modest alkyl spacer orientation and no main chain (carbonyl group) orientation was observed.<sup>[66]</sup> A longer spacer, compared to pDR1a, enabled the formation of LC phases, thanks to the decoupling concept,<sup>[67]</sup> but its flexibility accounts for the absence of orientation transfer from the azobenzene to the main chain.<sup>[66]</sup>

Supramolecular material design,<sup>[68]</sup> which employs spontaneously forming noncovalent bonds, such as hydrogen and halogen bonding, between photoactive azobenzenes and photopassive polymers, provides a window of opportunity to delve more deeply into the question of main chain vs. side group orientation, since it is easy to prepare supramolecular assemblies with variable spacer lengths, including spacer-free structures. By applying polarization modulation infrared structural absorbance spectroscopy (PM-IRSAS) - a method derived from PM-IRLD that, in addition, is capable of recording the absolute parallel and perpendicular absorbance spectra simultaneously, and thus can determine the structural absorbance spectrum and quantify the photo-orientation in situ<sup>[69]</sup> - we demonstrated that the larger photo-orientation of iodoacetylene-capped halogen-bonded azobenzenes compared to their hydrogen-bonded and non-bonded analogues leads to larger photo-orientation of the passive pyridine moiety of the poly(4-vinylpyridine) host but to no orientation of the main chain.<sup>[70]</sup> IR spectroscopy further allows distinguishing the occupied and free pyridine moieties in these supramolecularly bonded

complexes. Hence, by coupling a LED light ( $160 \text{ mW/cm}^2$  at  $450 \text{ nm}$ ) to static IR measurements, we showed that the supramolecular bonds are photostable enough (the high degree of supramolecular bonding is essentially unaffected by irradiation) to allow the partial transfer of the azo photo-orientation to the pyridine side group of the host polymer.<sup>[70]</sup> Cooperative orientation of the main chain was also reported for epoxy polymers containing spacer-free azobenzene side groups using polarized IR, but the main chain orientation was again found to be lower than that of the photoactive azo groups.<sup>[71]</sup>

Vibrational spectroscopy can likewise be used to study the kinetics of orientation and relaxation of the photoactive azobenzene groups as well as of the passive polymer moieties when orientation of the azo is partially transferred to the polymer. For pDR1a, the rate constants of azo and main chain orientation were found to be very similar, despite the main chain orientation being much smaller than that of the azo groups.<sup>[64, 65]</sup> This observation demonstrated that the “slow” and “fast” modes of biexponential kinetics of photo-orientation are not the consequence of motions of the main and side chains of the azopolymer, respectively, as previously thought,<sup>[72]</sup> but rather from different processes influencing each chemical group or to the existence of different molecular environments.<sup>[64, 65]</sup> For dispersed mixtures of the small molecule DR1 in different (isotactic, syndiotactic and atactic) poly(methyl methacrylate)s, it was shown that the host polymer with the lowest glass transition temperature ( $T_g$ ) ( $60 \text{ }^\circ\text{C}$ ) allowed the greatest DR1 mobility and thus the highest photo-orientation.<sup>[65]</sup> Recently, we have used PM-IRSAS to elucidate the  $T_g$  dependence of photo-orientation by mixing a DR1-containing molecular glass with various photopassive glasses.<sup>[73]</sup> We showed that the maximum orientation and the orientation stability, after the laser source is removed, are unaffected by the fraction of photoactive glass in the mixture at constant  $T_g$ . The orientation and orientation stability both increase with  $T_g$  up to an optimal value ( $60 \text{ }^\circ\text{C}$  for blends containing 40% of the photoactive glass) and then decrease and become constant, respectively, with further increase in the  $T_g$ , which helps explain the complex  $T_g$  dependence during the optical inscription of

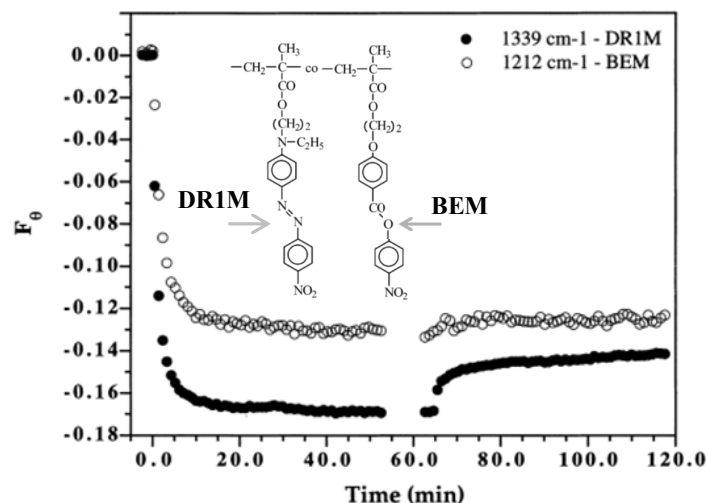
surface relief gratings.<sup>[73]</sup> Recent developments in molecular glass functionalization<sup>[74]</sup> may allow precise control of the molecular environment and thus enable a deeper understanding of photoinduced phenomena in azomaterials through IR investigations.

Photo-orientation studies of a methacrylate-based polymer bearing a less dipolar azobenzene side group than pDR1a provided valuable information about the mechanism of photo-orientation, where the long lifetime of the cis isomer allowed PM-IRLD to distinguish its orientational behavior independently of the trans isomer.<sup>[75]</sup> It was concluded that trans and cis orientation follow independent kinetics, that the cis isomer orients with its -N=N- bond preferentially parallel to the linear polarization direction, and that its anisotropy relaxes faster than the trans isomer after switching off the illumination. The latter was attributed to its globular geometry, which creates fewer constraints for rotational diffusion.<sup>[75]</sup>

Given that partial transfer the orientation of side-chain azobenzenes to a passive main chain is possible, a follow-up question addressable by vibrational spectroscopy is whether photoactive side-chain orientation can also be translated to a photopassive side chain in random copolymers containing azobenzene and non-azobenzene comonomers, so that the passive side chain contributes to the photoinduced birefringence. For one case, where the azo group has a very low dipole moment (0.04 D), it was shown that azobenzene photo-orientation occurs without orientation of the passive comonomer.<sup>[76]</sup> In other reported cases, for which the azobenzene comonomer had much a higher dipole moment, the photopassive comonomers were found to cooperatively orient with the azobenzene (as shown by the example in Figure 5 for a copolymer of photoactive DR1M and photopassive BEM monomers), whereas matching the dipole moments of the two comonomers remarkably enhances the orientation of the passive group.<sup>[77, 78]</sup> Thus, it was concluded that dipole-dipole interactions are the dominant mechanism compared to steric pushing/pulling for orienting photopassive molecules.<sup>[77]</sup> Being able to spectroscopically distinguish between the functional groups revealed that the two comonomers follow different orientation kinetics, with the azobenzene group described by biexponential and



the comonomer essentially by monoexponential kinetics, as illustrated in Figure 5.<sup>[78]</sup> This suggests that, unlike for the photoactive monomer, for which both AHB and angular redistribution contribute to photo-orientation, only one slower process dominates the orientation of the photopassive comonomer. Additionally, the passive comonomer groups were noted to retain most of their orientation after turning off the laser, whereas the orientation of the azobenzene-containing comonomer decreases due to thermal cis-trans isomerization and subsequent rotational diffusion.<sup>[78]</sup> Two-dimensional correlation IR spectroscopy can be used to establish the relative order of kinetic events and to increase spectral resolution in the asynchronous map.<sup>[79]</sup> This helped in distinguishing the contributions of the NO<sub>2</sub> symmetric stretching bands of the photoactive and photopassive comonomers and indicated that the photoactive DR1M units orient faster than the passive BEM, thus confirming the differences in the orientation behavior of the two comonomers.<sup>[80]</sup>



*Figure 5.* Orientation function under photo-orientation for photoactive DR1M and photopassive BEM moieties in a poly(DR1M-co-BEM) random copolymer (chemical structure shown) with a DR1M mole fraction of 0.52. Illumination began at 0 min and ceased at 60 min. Adapted with permission from Natansohn et al.<sup>[77]</sup> Copyright 1998. American Chemical Society.

The intrinsic order in semi-crystalline or liquid crystalline polymers, as compared to amorphous polymers, can increase the saturation value of their photoinduced anisotropy and improve the orientation stability once the irradiation is removed.<sup>[2]</sup> This was demonstrated for semi-crystalline polymers by Buffeteau and P  zolet, who compared an amorphous p(DR1a-co-MMA) copolymer and a semi-crystalline azopolymer whose rigid main chain contained phenylene diacrylate groups and onto which DR1-based side groups were directly attached with no intervening flexible spacer.<sup>[81]</sup> They found that the higher photoinduced anisotropy of semi-crystalline polymers is accompanied by biaxial orientation, in contrast to uniaxial orientation in the amorphous copolymer. In the biaxially oriented semi-crystalline polymer, the orientation of the azobenzene group was efficiently translated into orientation of the main chain, as probed using bands related to the phenylene groups which are spectrally isolated from the azo groups.<sup>[81]</sup> Photo-orientation studies of liquid crystalline polymers also showed a strong tendency to biaxial orientation under illumination.<sup>[82, 83]</sup> Additionally, polarized IR spectroscopy was used to show that the orientation of a passive benzoate comonomer is directly coupled to orientation of the azobenzene both below the  $T_g$  (glassy state) and above the  $T_g$  (nematic state).<sup>[82]</sup> Selective deuteration, which is a well-established method for isolating vibrational modes originating from different functional groups that would otherwise overlap and mask information in the IR and Raman spectra, was used for polyester-based liquid crystalline azopolymers to unambiguously distinguish the azobenzene orientation from the orientation of the alkyl spacer and the main chain, and a non-trivial dependence of the main chain orientation on the spacer length was found.<sup>[84]</sup> On the other hand, it was found that azobenzene orientation could be translated into main-chain orientation for a liquid crystalline polymer with a flexible aliphatic polyester backbone but not for the analogous polymer with a more rigid methyl methacrylate backbone.<sup>[85]</sup> These results underline that efficiently converting side-chain orientation to main-chain orientation is not trivial and requires well designed materials.

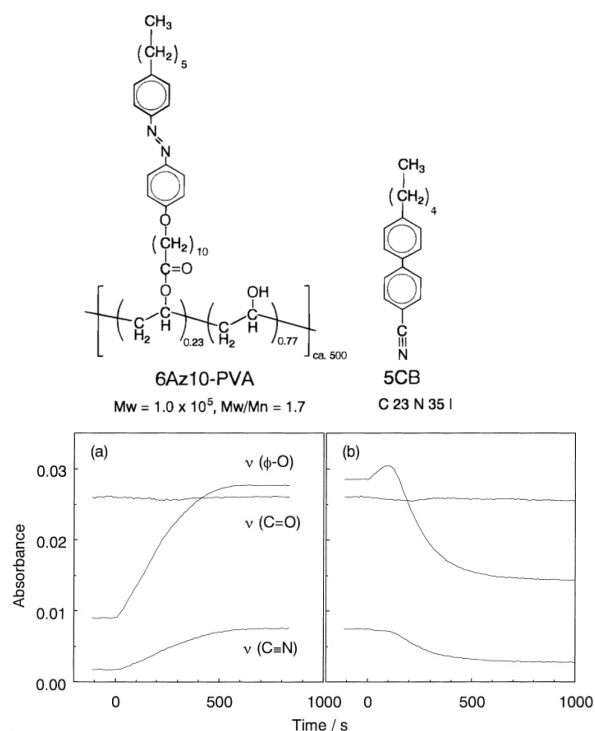


*Figure 6.* Chemical structures of an amphiphilic azo-containing copolymer and the 5CB liquid crystal (top). IR absorbance of selected bands as a function of time upon trans-to-cis isomerization (366 nm light, bottom left panel) and cis-to-trans isomerization (436 nm light, bottom right panel) of a stack of 49 Langmuir-Blodgett layers of the polymer and 5CB in equimolar proportion relative to the azo-containing repeat unit. Reproduced with permission from Ubukata et al.<sup>[86]</sup> Copyright 2001. American Chemical Society.

As already illustrated in Figure 1b, the photoinduced anisotropy of azopolymers can be put to good use as command layers, in which the orientation of a thick layer of liquid crystals ("soldiers") is controlled by the photoresponse of a thin azopolymer layer ("commander"), typically located next to the substrate below the LC layer but more recently shown to be applicable as well at the free surface.<sup>[22]</sup> Mixed multilayers of an amphiphilic azopolymer and a well-studied liquid crystal, 5CB, depicted in Figure 6, were prepared using the Langmuir-Blodgett technique in order to mimic the interfacial region between the command surface and the LC phase.<sup>[86]</sup> IR spectroscopy in the transmission and the reflection-absorption (IRRAS) modes were combined to provide information on both in-plane and out-of-plane molecular

anisotropy. Because of the surface selection rule of IRRAS, this technique is highly sensitive to vibrational modes perpendicular to the surface.<sup>[39]</sup> The initial ultrathin films presented homeotropic orientation for both the azo group and 5CB. As shown in Figure 6 (bottom left panel), in situ irradiation with 366 nm UV light led to the reorientation of both the azobenzene (using a phenyl-O-C stretching band) and 5CB (using the nitrile stretching band) from perpendicular to tilted orientation, in agreement with UV-visible results. The chemical selectivity of IR also allowed concluding that there was no effect on the main chain, given the absence of change in the C=O stretching band absorbance, again confirming that a long and flexible spacer (alkyl chain of 10 methylene units) efficiently decouples the main chain from the azobenzene. Kinetic analysis of the IR data showed that the reorientation of the azo proceeds faster than for 5CB. The reverse process, from tilted to homeotropic alignment, was conducted using 436 nm visible light (bottom right panel of Fig. 6) and revealed that a threshold of azobenzene cis-trans conversion, reached after 150 s at this irradiance, is needed to induce a change in 5CB orientation. Both the homeotropic-tilted and tilted-homeotropic transitions could be accelerated by increasing the irradiance of the illuminating light.<sup>[86]</sup> Later, Ohe et al. demonstrated the power of vibrational sum frequency generation (SFG) spectroscopy in resolving the molecular orientation of the same azopolymer at the air-water interface. In particular, it was found that the trans isomers orient perpendicularly to the surface while the cis isomers are parallel to the surface, and that the orientation of both is affected by the surface pressure.<sup>[87]</sup>

To summarize, the chemical selectivity and time resolution of polarized IR spectroscopy has enabled resolving the orientation kinetics of individual molecular moieties in real time and revealed several aspects of the complex phenomena associated with the photoinduced orientation of azomaterials. Surface selective methods such as IRRAS and SFG enable studying anisotropy in thin films down to monolayer thicknesses and should see increased use in the future. We also emphasize that polarized Raman spectroscopy, although much less commonly

employed, has some clear advantages over IR methods when measuring samples in small quantities or in shapes such as nm-sized electrospun fibers,<sup>[88]</sup> as demonstrated by recent examples of polarized photopolymerization-induced order<sup>[89]</sup> and azobenzene orientation within the shells of vesicles.<sup>[90]</sup> Additionally, Raman spectroscopy enables solving more complex orientation distributions and provides the spatial resolution for probing depth-dependent orientation in cases where the photo-orientation and cis content depend strongly on the penetration of light in thick materials, for instance in self-standing films undergoing photoinduced bending and in light-powered cantilever actuators.<sup>[25, 91-93]</sup> Consequently, we expect polarized Raman to play an increasingly important role in future studies.

#### **4. Photoinduced chirality**

Vibrational optical activity, which is measured as the difference in the absorbance of left- and right-handed circularly polarized IR light (vibrational circular dichroism, VCD) or as the difference in Raman intensity (Raman optical activity, ROA) between the two incident circular polarizations and/or the two scattered polarizations, provides information on the chiral character of single molecules or supramolecular assemblies of many molecules.<sup>[94]</sup> As for linear dichroism, the interest of vibrational optical activity stems from the higher structural information that can be gathered in comparison to electronic transitions in the UV-visible range thanks to the selectivity of vibrational modes to specific moieties or components in complex systems.<sup>[94]</sup> When coupled with suitable computational support (usually DFT ab initio calculations), these techniques can solve the absolute configuration of chiral organic molecules<sup>[95]</sup> and elucidate what structural units give rise to optical activity in supramolecular chiral structures.<sup>[96]</sup>

Azobenzene photoisomerization has already been used in chiroptical switching, where the optical activity stems from the supramolecular self-assembly of macromolecules<sup>[97]</sup> or from intrinsically chiral helical structures.<sup>[17]</sup> Iftime et al. demonstrated that an initially achiral

smectic A liquid crystalline azopolymer can be used as a chiroptical switch, for which illumination with circularly polarized light induces chirality whose handedness can be switched by selecting the handedness of the illuminating light.<sup>[98]</sup> The authors mentioned that using VCD would be crucial for separating the contributions of the polymer main chain and azobenzene to the induced chirality. However, considering that no main-chain orientation was observed by PM-IRLD for this polymer upon photo-orientation,<sup>[66]</sup> attributed to the flexibility of the spacer, one can expect that VCD or ROA would reveal light-induced chirality only for the azo side chains.

For an initially achiral nematic liquid crystalline azopolymer, whose structure is shown in Figure 7b, photoinduced chiral nematic order was similarly demonstrated, with the proposed mechanism depicted in Figure 7a.<sup>[99]</sup> The enantiomeric supramolecular helices, identified by electronic circular dichroism, were found to be stable for at least two months after switching off the illumination. The authors found that only vibrational bands assigned to azobenzenes show a VCD response (see VCD spectra in the upper panel of Figure 7b), whereas the C=O stretching band ( $1725\text{ cm}^{-1}$ ) of the ester group located near the backbone, which has medium intensity in the normal IR absorbance spectrum (lower panel of Figure 7b), is completely VCD-silent, thus showing that the supramolecular chirality is due to the organization of the azobenzene side chains into a chiral structure upon illumination by circularly polarized light.<sup>[99]</sup> An analogous induction of photoinduced chirality was found in supramolecular columnar liquid crystals, leading to a qualitatively similar conclusion.<sup>[100]</sup>

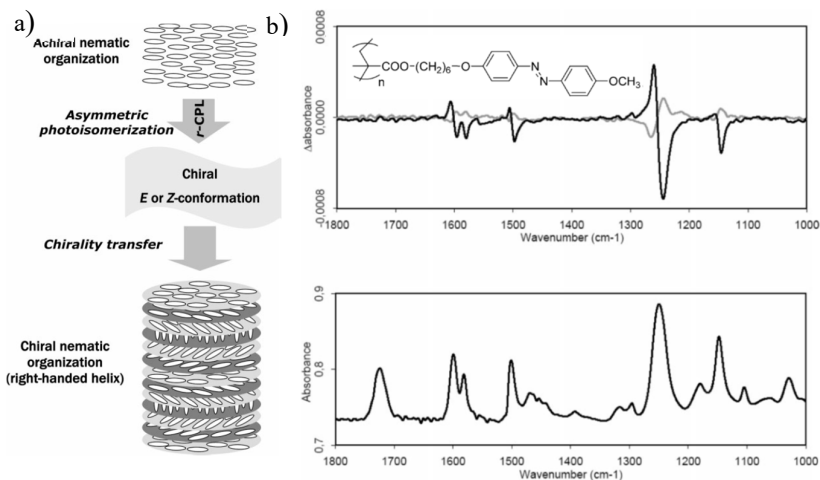


*Figure 7:* a) Schematic representation of photoinduced chirality in an achiral nematic liquid crystalline azopolymer by illumination with circularly polarized light. Chiroptical switching was realized by changing the handedness of the circularly polarized light. b) VCD spectra upon illumination of right-handed (black) and left-handed (grey) circularly polarized light (top panel) and normal IR absorbance spectrum (bottom panel) of the liquid crystalline azobenzene polymer shown. Adapted with permission from Tejedor et al.<sup>[99]</sup> Copyright 2007. Wiley-VCH, Weinheim.

VCD has also been shown to be a powerful tool for studies of photoinduced folding/unfolding of helical foldamers, given that the helical secondary structures exhibit chirality. In a recent example, the vibrational circular dichroism of N=N stretching bands in an azobenzene-containing foldamer backbone were shown to be good markers for determining the conformation of the foldamer upon photoinduced unfolding and helicity changes.<sup>[101]</sup> We believe that more extensive use of vibrational optical activity may increase understanding of the role of each molecular moiety and thus help to improve the design of switchable chiral structures of molecules and supramolecular assemblies, both in solution and in the solid state.

## 5. All-optical mass transport of material

One of the most remarkable consequences of azobenzene photoisomerization is optically driven mass transport of material that occurs at the micrometer scale under irradiation with an intensity

or polarization gradient, often in the form of an interference pattern. Depending on the shape and nature of the light pattern incident on the azopolymer film, different surface structures such as sinusoidal gratings (often referred to as surface relief gratings (SRGs)), 2D egg-shell gratings, craters and spirals can be created, as depicted in Figure 8.<sup>[21, 102, 103]</sup> Even more complicated spatially varying structures are possible through polarization sensitive directional photofluidization lithography<sup>[20]</sup> as well as sequential steps of writing and partial erasure of these surface patterns.<sup>[104]</sup> The application prospects of these structures range from photonics components, such as waveguide couplers, to micro- and nanoscale templating tools and even to cell culture substrates.<sup>[60, 105, 106]</sup> All-optical surface patterning was demonstrated for different types of azomaterials including amorphous<sup>[2]</sup> and liquid crystalline<sup>[3]</sup> side-chain azopolymers, molecular glasses<sup>[107, 108]</sup> and supramolecular polymer-azobenzene complexes.<sup>[109, 110]</sup> Surface pattern formation can also occur under illumination by a single polarized beam, in so-called spontaneous surface patterning,<sup>[107, 111]</sup> and at temperatures down to at least 73 K (the lowest temperature tested to our knowledge),<sup>[112]</sup> which can reveal information about the early stages of the pattern formation due to the slower kinetics at low temperature.

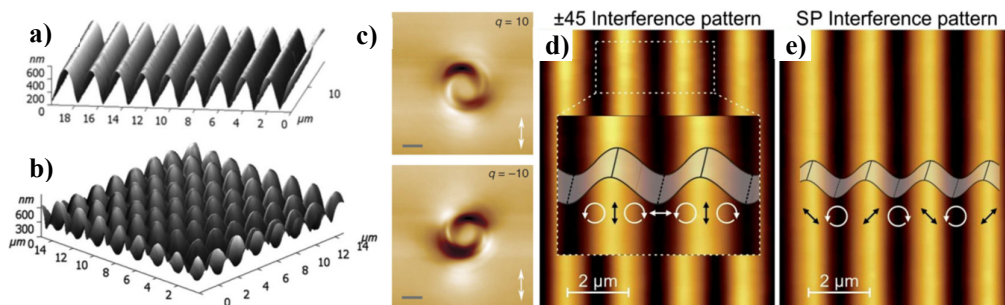


*Figure 8:* AFM micrographs of a) sinusoidal, b) egg-shell, and c) spiral photoinduced patterns. The distribution of the electrical field vector relative to the position of the maxima and minima of the sinusoidal SRGs prepared using d)  $\pm 45^\circ$  and e) sp interference patterns. Panels a and b reproduced with permission from Goldenberg et al.<sup>[103]</sup> Copyright 2009. Royal Society of Chemistry. Panel c reproduced with permission from Ambrosio et al.<sup>[102]</sup> Copyright 2012. Nature Publishing Group. Panels d and e reproduced with permission from Di Florio et al.<sup>[113]</sup> Copyright 2014. Royal Society of Chemistry.



Even though the phenomenon was discovered more than 20 years ago,<sup>[114, 115]</sup> the community is still debating the mechanisms behind this massive molecular motion below  $T_g$  under illumination, the only consensus reached thus far being that azobenzene photoisomerization is required for the process to take place.<sup>[116]</sup> A qualitatively similar but mechanistically different (essentially thermal) all-optical surface patterning phenomenon occurring in LC polymers, where illumination above  $T_g$  leads to a LC phase transition, should not be associated with this debate.<sup>[3]</sup> In situ near-field optical microscopy was used to show that there are at least two mechanisms (intensity- and polarization-induced) with distinctly different kinetics leading to mass transport for amorphous pDR1a.<sup>[117]</sup> Other recent experimental observations also support the coexistence of at least two mechanisms,<sup>[118]</sup> one related to photo-orientation induced stresses in the material<sup>[119-122]</sup> and the other to isomerization-induced dynamic heterogeneities driving local diffusion-like motion of the molecules.<sup>[116, 123-126]</sup>

Vibrational spectroscopy can contribute to the debate because it can measure both photo-orientation and photoinduced changes in the molecular environment. Polarized confocal Raman microscopy provides a spatial resolution at the same scale as the surface undulation resulting from a two-beam interference pattern and thus enables probing the orientation distribution of the molecules in different sections of a SRG. Sourisseau and coworkers were pioneers in this field, developing the formalisms to deduce the orientation distribution from polarized Raman signals.<sup>[127]</sup> They have shown that the orientation distribution of the chromophores varies spatially along the grating (i.e. whether on a hill, slope or valley) and depends on the polarization combination used for the interfering beams. They concluded that the orientation of the chromophores is not only dictated by the spatially varying polarization of the incident irradiation but also by the mass transport of the polymer chains.<sup>[128-130]</sup> They also reported differences in dye concentration between the hills and the valleys of a SRG.<sup>[131]</sup> They took advantage of preresonant conditions to enhance the intensity of azo-related bands but did not

report on the orientation of the polymer main chain, which still remains an open question especially in view of its common decoupling from the orientation of the azo side groups as discussed in Section 3. Later, they demonstrated that a SRG can be poled by an electric dc field to increase polar ordering of the azobenzenes, as characterized by second harmonic generation near-field scanning optical microscopy (at visible wavelengths) combined with confocal Raman microscopy.<sup>[132]</sup> The polar ordering was found to be larger on the hills and especially on the slopes, as compared to lower values for the valleys of the surface structure.

The formalism developed by Sourisseau and coworkers was further applied by Havenith and coworkers to study the chromophore orientation at different locations of SRGs prepared using various interference patterns.<sup>[113]</sup> Among these, they found anisotropic orientation distributions in the areas subjected to circular polarization under a  $\pm 45^\circ$  interference pattern, suggesting that the mass transport itself contributes to the orientation (uniform illumination with circular polarization maintaining in-plane isotropy, as discussed in Section 3). They used lateral sectioning of the gratings to show that anisotropy penetrates the entire polymer film and is not restricted to its illuminated surface, although it should be noted that the reported orientation parameters were modest. They also successfully adsorbed graphene onto the azopolymer surface<sup>[133]</sup> and used the well-known shift of the Raman G-band as direct evidence of stress induced in the adsorbed graphene due to the mass transport of the underlying azopolymer.<sup>[134]</sup> The stress level was calculated to reach above 1 GPa, indicating that the azopolymer remains glassy under irradiation as opposed to reaching a fluid-like state. To contextualize this observation, UV-visible and Raman spectroscopy measurements on pDR1a have shown that the fraction of cis isomers in the photostationary state decreases when applying an increasing hydrostatic pressure but that some photoisomerization remains possible even at applied pressures as high as 1 GPa.<sup>[135]</sup> This capability of macroscopic material transport can be used to move passive objects, as was shown for polystyrene nanoparticles on the surface of an azobenzene-containing glassy film.<sup>[136]</sup>

Recently, tip-enhanced Raman scattering (TERS), a technique that provides a spatial resolution well below the diffraction limit, down to 1-2 nm,<sup>[137]</sup> was used to characterize the 3D orientation of an azopolymer. It was reported that homeotropic and planar orientations of the azo side-chains can be obtained by applying a dc electric field with an AFM tip and a near-field longitudinal resonant light, respectively.<sup>[138]</sup> By taking advantage of the exquisite sensitivity of TERS, it was even possible to observe the reversible cis-trans photoisomerization of a single azobenzene molecule.<sup>[139]</sup>

While vibrational spectroscopy is normally used to obtain information on the azopolymer behavior, the roles can sometimes be reversed. Indeed, surface-enhanced Raman scattering (SERS) and IR absorption (SEIRA) depend on the strong electric field enhancement created by plasmonic structures and especially by the presence of hot spots between nanoparticles. AFM was used to image, with nanoscale resolution, the impact of irradiation on the localization of azopolymers deposited on such plasmonic structures, helping to optimize the design of substrates for surface-enhanced spectroscopy.<sup>[140, 141]</sup> Both SERS and TERS were also shown to be powerful tools for catalyzing the coupling of amino- or nitro-phenol functionalized molecules to form the corresponding azobenzene thanks to the high energy of hot electrons originating from localized surface plasmons. It was further demonstrated very recently that the scanning capabilities and plasmon confinement properties of a TERS tip enable extending this concept to bifunctionalized molecules to create main-chain azopolymers at the micron scale, but with nanometer scale control of the polymerization process.<sup>[142]</sup>

By employing attenuated total reflection IR spectroscopy with in situ heating and illumination, we have characterized the photoinduced changes in the molecular environment of pDR1a and of a DR1-containing mexylaminotriazine molecular glass, the structures of which are shown in Figure 9a.<sup>[143]</sup> Figure 9b shows that IR bands associated with the azo group shift as a function of temperature, enabling determination of the  $T_g$  spectroscopically. It was found that the  $T_g$  is unaffected by irradiation, but that the molecular environment of the azo is highly perturbed by

cyclic illumination (2 min on, 2 min off). The similarity of the band shifts under irradiation and heating allowed defining an "effective temperature" as that to which the material should be heated in order to reproduce the light-induced effect. The effective temperature, reflecting the photoinduced perturbation of molecular environment, was shown to depend strongly on the molecular location of the moieties, with the azo group the most highly perturbed and, at the other extreme, the glass core or polymer backbone completely unaffected by irradiation in the two materials studied. These results suggest the existence of sub-molecular dynamic heterogeneities that contribute to the photoinduced mass transport in azomaterials.<sup>[143]</sup> It is noteworthy that unpolarized LED light was used, which should minimize orientation-induced stresses in the materials.

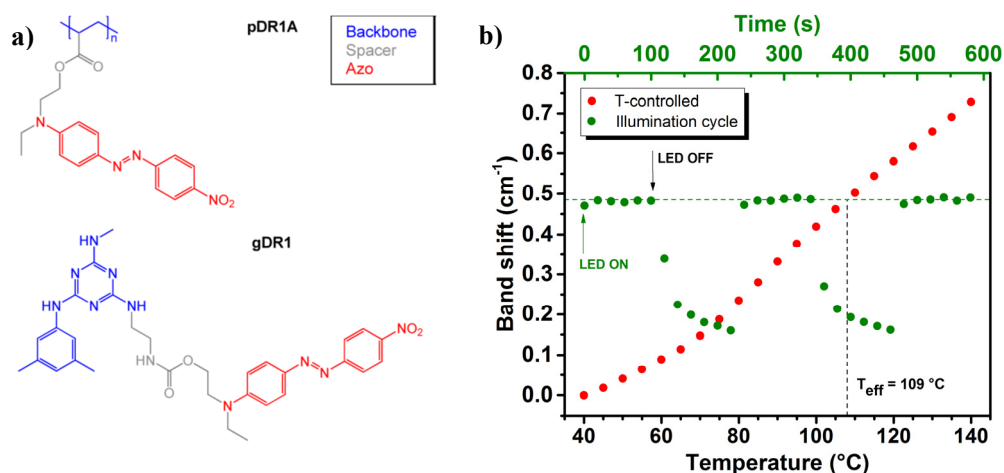


*Figure 9:* Molecular structures of pDR1a and of an azobenzene-containing molecular glass (gDR1) showing the azobenzene (red), spacer (gray) and backbone (blue) moieties. b) Determination of the effective temperature by comparing the band shift measured under cyclic illumination (120 s lights on, 120 s lights off; green data) at constant temperature to the band shifts as a function of temperature without irradiation (red data). A large increase of effective temperature was found for the azo bands (illustrated here for the symmetric NO<sub>2</sub> stretching vibration of gDR1) while no increase was found for the backbone bands. Adapted with permission from Vapaavuori et al.<sup>[143]</sup> Copyright 2015. American Chemical Society.

Despite the knowledge gained from studying SRGs prepared with patterned illumination and the related photo-orientation under uniform illumination (reviewed in Section 3), there are still many unanswered questions regarding light-induced transport and photomobility in azomaterials. For example, the orientation values measured for SRGs are well below the theoretical maximum and are lower than the values obtained using a single polarized irradiation source. Care must also be taken not to assume that the azobenzene orientation reflects the orientation of the polymer main chain. Moreover, only modest main chain orientation is observed by PM-IRLD for pDR1a despite its capability of creating SRGs with high diffraction efficiency. To our knowledge, there are no studies directly comparing the photo-orientation under identical material and experimental conditions, such as irradiation intensity, wavelength and time interval between inscription and analysis. Further studies exploiting the chemical sensitivity of polarized Raman microscopy and other spatially resolved spectroscopy techniques to determine the orientation distribution function of different molecular groups in SRGs are therefore desirable. Future work of interest also comprises the extension of the IR-based photomobility and photo-orientation studies to supramolecular polymer-azobenzene complexes, which have shown the capacity of producing photoinduced SRGs even at very low azobenzene content (and thus low global orientation).<sup>[144]</sup> Developments in various near-field techniques, both in IR and Raman, will open up new avenues for characterization and manipulation of photomobile materials at spatial resolutions well below the optical diffraction limit.

## **6. Conclusion and outlook**

Photoinduced molecular-level geometrical changes in light-powered molecular switches and motors can lead to significant bulk-level material motions and changes in functional properties when these light-active molecules are coupled to macromolecules. To advance the understanding of these important photoinduced phenomena, vibrational spectroscopy provides

complementary advantages to other contemporary material characterization methods, in particular because of its chemical selectivity that allows distinguishing the photoresponse of specific chemical groups, its flexibility in handling different sample types (from bulk materials to monolayers and even individual molecules), its easy coupling with illumination sources for in situ studies, and its capacity to probe orientation and chiral order. While the most advanced techniques, such as fs time-resolved spectroscopy, coherent 2D-IR spectroscopy, sum frequency generation and near-field vibrational spectroscopies, remain the domains of specialized laboratories, several methods highlighted in this feature article, such as confocal Raman microscopy and polarized IR spectroscopy, are accessible to the majority of materials and polymer scientists.

A general observation throughout the reviewed studies is that the mechanisms by which the photoisomerization of azobenzene is coupled to changes in the macromolecular and/or material structure, whether it is the folding or unfolding of a peptide, the photoinduced chirality in LC azopolymers, or the mass transport of illuminated azomaterials, are not straightforward and not yet fully understood. As one example, the photo-orientation or chiral order of the azobenzene and of the polymer backbone to which it is attached are usually very different, as was also the case for photoinduced changes in the molecular environment in the vicinity of the azobenzene versus the vicinity of the backbone moieties. Indeed, the flexible parts in the molecules commonly appear to moderate, or even completely absorb, the abrupt changes experienced by the azobenzene. These azopolymers can nevertheless undergo large-scale motions and structural reorganization, indicating that such phenomena in photonic materials are more subtle than revealed by more commonly used techniques for characterizing azopolymers, such as UV-visible spectroscopy and birefringence.

In this context, the chemical selectivity of vibrational spectroscopy can emphasize the importance of small structural differences and thereby guide the polymer scientist in optimizing the molecular design of azomaterials. For instance, applying Raman spectroscopy to distinguish

the orientation of the macromolecular backbone from the azobenzene moiety along the pitch of SRGs and to probe photo-orientation at different depths in LC polymer actuators (where functionality arises from the decreasing light penetration with depth) should lead to a better control and design of such systems. Near-field methods, such as tip-enhanced Raman scattering, photothermal induced resonance and scattering infrared near-field scanning optical microscopy, can provide spatial resolutions well below the diffraction limit<sup>[137, 145, 146]</sup> and, although they have seldom been applied to azomaterials, their increasing availability offers appealing prospects.

While this article focused on azobenzene-based materials, one of its aims was to raise awareness of the versatility and power of vibrational spectroscopy techniques for characterizing photoinduced changes in photoswitchable macromolecules in general. Furthermore, vibrational spectroscopy is certainly not restricted to responses induced by photoswitching, but can also be an effective tool for investigating other stimuli-induced switching, such as through electric fields, pH and temperature.

## **Appendix/Nomenclature/Abbreviations**

This work was supported by the Natural Sciences and Engineering Research Council of Canada (NSERC). JV acknowledges a Banting Postdoctoral Fellowship for generous financial support. We thank F. Laguné-Labarthe for discussions and help with graphic design.

Received: Month XX, XXXX; Revised: Month XX, XXXX; Published online:

Keywords: azopolymers; vibrational spectroscopy; photoisomerization; photoinduced anisotropy; surface relief grating.

## References

- [1] Y. Zhao, T. Ikeda, "Smart Light-Responsive Materials: Azobenzene-Containing Polymers and Liquid Crystals", John Wiley & Sons, Inc., New York, NY, USA, 2009.
- [2] A. Natansohn, P. Rochon, *Chem. Rev.* **2002**, *102*, 4139.
- [3] T. Seki, *Macromol Rapid Commun.* **2014**, *35*, 271.
- [4] A. A. Beharry, G. A. Woolley, *Chem. Soc. Rev.* **2011**, *40*, 4422.
- [5] W. Szymanski, J. M. Beierle, H. A. Kistemaker, W. A. Velema, B. L. Feringa, *Chem. Rev.* **2013**, *113*, 6114.
- [6] T. Ly, R. R. Julian, *Angew. Chem. Int. Ed.* **2009**, *48*, 7130.
- [7] S. Dadashi-Silab, S. Doran, Y. Yagci, *Chem. Rev.* **2016**, *116*, 10212.
- [8] H. Tian, S. Yang, *Chem. Soc. Rev.* **2004**, *33*, 85.
- [9] M. Irie, T. Fukaminato, K. Matsuda, S. Kobatake, *Chem. Rev.* **2014**, *114*, 12174.
- [10] H. Bouas-Laurent, H. Dürr, *Pure Appl. Chem.* **2001**, *73*.
- [11] P. Bodis, M. R. Panman, B. H. Bakker, A. Mateo-Alonso, M. Prato, W. J. Buma, A. M. Brouwer, E. R. Kay, D. A. Leigh, S. Woutersen, *Acc. Chem. Res.* **2009**, *42*, 1462.
- [12] D. Brinks, R. Hildner, E. M. van Dijk, F. D. Stefani, J. B. Nieder, J. Hernando, N. F. van Hulst, *Chem. Soc. Rev.* **2014**, *43*, 2476.
- [13] A. B. Elliott, R. Horvath, K. C. Gordon, *Chem. Soc. Rev.* **2012**, *41*, 1929.
- [14] X. Zhang, L. Hou, P. Samori, *Nat. Commun.* **2016**, *7*, 11118.
- [15] H. M. Bandara, S. C. Burdette, *Chem. Soc. Rev.* **2012**, *41*, 1809.
- [16] D. Bleger, S. Hecht, *Angew. Chem. Int. Ed.* **2015**, *54*, 11338.
- [17] G. A. Woolley, *Acc. Chem. Res.* **2005**, *38*, 486.
- [18] T. Ikeda, S. Horiuchi, D. B. Karanjit, S. Kurihara, S. Tazuke, *Macromolecules* **1990**, *23*, 42.
- [19] H. Zhou, C. Xue, P. Weis, Y. Suzuki, S. Huang, K. Koynov, G. K. Auernhammer, R. Berger, H. J. Butt, S. Wu, *Nat. Chem.* **2017**, *9*, 145.
- [20] S. Lee, H. S. Kang, J. K. Park, *Adv. Mater.* **2012**, *24*, 2069.
- [21] N. K. Viswanathan, D. Y. Kim, S. Bian, J. Williams, W. Liu, L. Li, L. Samuelson, J. Kumar, S. K. Tripathy, *J. Mater. Chem.* **1999**, *9*, 1941.
- [22] T. Seki, *Polym. J.* **2014**, *46*, 751.
- [23] S. Iamsaard, S. J. Asshoff, B. Matt, T. Kudernac, J. J. Cornelissen, S. P. Fletcher, N. Katsonis, *Nat. Chem.* **2014**, *6*, 229.
- [24] S. Serak, N. Tabiryan, R. Vergara, T. J. White, R. A. Vaia, T. J. Bunning, *Soft Matter* **2010**, *6*, 779.
- [25] K. Kumar, C. Knie, D. Bleger, M. A. Peletier, H. Friedrich, S. Hecht, D. J. Broer, M. G. Debije, A. P. Schenning, *Nat. Commun.* **2016**, *7*, 11975.
- [26] R. J. Moerland, J. E. Koskela, A. Kravchenko, M. Simberg, S. van der Vegte, M. Kaivola, A. Priimagi, R. H. A. Ras, *Mater. Horiz.* **2014**, *1*, 74.
- [27] L. M. Goldenberg, V. Lisinetskii, Y. Gritsai, J. Stumpe, S. Schrader, *Adv. Mater.* **2012**, *24*, 3339.
- [28] L. M. Goldenberg, V. Lisinetskii, S. Schrader, *Adv. Opt. Mater.* **2013**, *1*, 527.
- [29] J. M. Chalmers, "Mid-Infrared Spectroscopy of the Condensed Phase", in *Handbook of Vibrational Spectroscopy*, J.M. Chalmers and P.R. Griffiths, Eds., John Wiley & Sons, Ltd, Chichester, U.K., 2002, p. 128.
- [30] N. J. Everall, "Raman Spectroscopy of the Condensed Phase", in *Handbook of Vibrational Spectroscopy*, J.M. Chalmers and P.R. Griffiths, Eds., John Wiley & Sons, Ltd, Chichester, U.K., 2002, p. 141.
- [31] R. Bhargava, I. W. Levin, *Macromolecules* **2003**, *36*, 92.
- [32] K. L. A. Chan, S. G. Kazarian, *Chem. Soc. Rev.* **2016**, *45*, 1850.



- [33] R. Salzer, H. W. Siesler, *"Infrared and Raman Spectroscopic Imaging"*, Wiley-VCH, New York City, NY, 2009.
- [34] C. Findlay, J. Morrison, C. J. Mundy, J. Sedlmair, C. J. Hirschmugl, K. M. Gough, *Analyst* **2017**, *142*, 660.
- [35] C. R. Findlay, R. Wiens, M. Rak, J. Sedlmair, C. J. Hirschmugl, J. Morrison, C. J. Mundy, M. Kansiz, K. M. Gough, *Analyst* **2015**, *140*, 2493.
- [36] R. K. Reddy, M. J. Walsh, M. V. Schulmerich, P. S. Carney, R. Bhargava, *Appl. Spectrosc.* **2013**, *67*, 93.
- [37] N. J. Everall, *Appl. Spectrosc.* **2000**, *54*, 1515.
- [38] N. J. Everall, *Appl. Spectrosc.* **2009**, *63*, 245A.
- [39] J. Umemura, "Reflection–Absorption Spectroscopy of Thin Films on Metallic Substrates", in *Handbook of Vibrational Spectroscopy*, J.M. Chalmers and P.R. Griffiths, Eds., John Wiley & Sons, Ltd, Chichester, U.K., 2002, p. 982.
- [40] W. E. Smith, *Chem. Soc. Rev.* **2008**, *37*, 955.
- [41] Z. Chen, Y. R. Shen, G. A. Somorjai, *Annu. Rev. Phys. Chem.* **2002**, *53*, 437.
- [42] M. Quick, A. L. Dobryakov, M. Gerecke, C. Richter, F. Berndt, I. N. Ioffe, A. A. Granovsky, R. Mahrwald, N. P. Ernsting, S. A. Kovalenko, *J. Phys. Chem. B* **2014**, *118*, 8756.
- [43] C. Renner, L. Moroder, *ChemBioChem* **2006**, *7*, 868.
- [44] R. J. Mart, R. K. Allemann, *Chem. Commun.* **2016**, *52*, 12262.
- [45] Z. Yu, S. Hecht, *Chem. Commun.* **2016**, *52*, 6639.
- [46] S. Krimm, J. Bandekar, *Adv. Protein Chem.* **1986**, *38*, 181.
- [47] J. Bredenbeck, J. Helbing, A. Sieg, T. Schrader, W. Zinth, C. Renner, R. Behrendt, L. Moroder, J. Wachtveitl, P. Hamm, *Proc. Natl. Acad. Sci. U.S.A.* **2003**, *100*, 6452.
- [48] J. A. Ihalainen, B. Paoli, S. Muff, E. H. Backus, J. Bredenbeck, G. A. Woolley, A. Caflisch, P. Hamm, *Proc. Natl. Acad. Sci. U.S.A.* **2008**, *105*, 9588.
- [49] J. Bredenbeck, J. Helbing, J. R. Kumita, G. A. Woolley, P. Hamm, *Proc. Natl. Acad. Sci. U.S.A.* **2005**, *102*, 2379.
- [50] T. E. Schrader, T. Cordes, W. J. Schreier, F. O. Koller, S. L. Dong, L. Moroder, W. Zinth, *J. Phys. Chem. B* **2011**, *115*, 5219.
- [51] S. Steinwand, Z. Yu, S. Hecht, J. Wachtveitl, *J. Am. Chem. Soc.* **2016**, *138*, 12997.
- [52] P. Hamm, J. Helbing, J. Bredenbeck, *Annu. Rev. Phys. Chem.* **2008**, *59*, 291.
- [53] M.-H. Li, P. Keller, *Soft Matter* **2009**, *5*, 927.
- [54] K. Chen, G. Xue, G. Shen, J. Cai, G. Zou, Y. Li, Q. Zhang, *RSC Adv.* **2013**, *3*, 8208.
- [55] G. Shen, G. Xue, J. Cai, G. Zou, Y. Li, M. Zhong, Q. Zhang, *Soft Matter* **2012**, *8*, 9127.
- [56] G. Shen, G. Xue, J. Cai, G. Zou, Y. Li, Q. Zhang, *Soft Matter* **2013**, *9*, 2512.
- [57] Z. K. Cui, T. Phoeung, P. A. Rousseau, G. Rydzek, Q. Zhang, C. G. Bazuin, M. Lafleur, *Langmuir* **2014**, *30*, 10818.
- [58] J. A. Delaire, K. Nakatani, *Chem. Rev.* **2000**, *100*, 1817.
- [59] Z. Sekkat, J. Wood, W. Knoll, *J. Phys. Chem.* **1995**, *99*, 17226.
- [60] A. Natansohn, P. Rochon, *Adv. Mater.* **1999**, *11*, 1387.
- [61] D. R. Robello, P. T. Dao, J. S. Schildkraut, M. Scozzafava, E. J. Urankar, C. S. Willand, *Chem. Mater.* **1995**, *7*, 284.
- [62] T. Seki, H. Fukumoto, M. Hara, N. Kawatsuki, S. Nagano, *J. Ceram. Soc. Jpn.* **2008**, *116*, 361.
- [63] T. Seki, M. Sakuragi, Y. Kawanishi, T. Tamaki, R. Fukuda, K. Ichimura, Y. Suzuki, *Langmuir* **1993**, *9*, 211.
- [64] T. Buffeteau, M. Pézolet, *Appl. Spectrosc.* **1996**, *50*, 948.
- [65] T. Buffeteau, F. Lagugné Labarthe, M. Pézolet, C. Sourisseau, *Macromolecules* **1998**, *31*, 7312.
- [66] F. Lagugné Labarthe, S. Freiberg, C. Pellerin, M. Pézolet, A. Natansohn, P. Rochon, *Macromolecules* **2000**, *33*, 6815.

- [67] H. Finkelmann, H. Ringsdorf, J. H. Wendorff, *Makromol. Chem.* **1978**, 179, 273.
- [68] P. A. Gale, J. W. Steed, "Supramolecular Chemistry: From Molecules to Nanomaterials", John Wiley and Sons, Inc, 2012, 10.1002/97804706613454014.
- [69] Y. Liang, D. Mauran, R. E. Prud'homme, C. Pellerin, *Appl. Spectrosc.* **2008**, 62, 941.
- [70] J. Vapaavuori, I. T. S. Heikkinen, V. Dichiarante, G. Resnati, P. Metrangolo, R. G. Sabat, C. G. Bazuin, A. Priimagi, C. Pellerin, *Macromolecules* **2015**, 48, 7535.
- [71] Y. Wang, Y. He, X. Wang, *Polym. Bull.* **2011**, 68, 1731.
- [72] D. Brown, A. Natansohn, P. Rochon, *Macromolecules* **1995**, 28, 6116.
- [73] A. Laventure, J. Bourotte, J. Vapaavuori, L. Karperien, R. G. Sabat, O. Lebel, C. Pellerin, *ACS Appl. Mater. Interfaces* **2017**, 9, 798.
- [74] O. R. Bannani, T. A. Al-Hujran, J.-M. Nunzi, R. G. Sabat, O. Lebel, *New J. Chem.* **2015**, 39, 9162.
- [75] T. Buffeteau, F. Lagugné Labarthe, M. Pézolet, C. Sourisseau, *Macromolecules* **2001**, 34, 7514.
- [76] K. Anderle, R. Birenheide, M. J. A. Werner, J. H. Wendorff, *Liq. Cryst.* **1991**, 9, 691.
- [77] A. Natansohn, P. Rochon, X. Meng, C. Barrett, T. Buffeteau, S. Bonenfant, M. Pézolet, *Macromolecules* **1998**, 31, 1155.
- [78] T. Buffeteau, A. Natansohn, P. Rochon, M. Pézolet, *Macromolecules* **1996**, 29, 8783.
- [79] I. Noda, A. E. Dowrey, C. Marcoli, G. M. Story, Y. Ozaki, *Appl. Spectrosc.* **2000**, 54, 236.
- [80] M. Pézolet, C. Pellerin, R. E. Prud'homme, T. Buffeteau, *Vib. Spectrosc.* **1998**, 18, 103.
- [81] T. Buffeteau, M. Pézolet, *Macromolecules* **1998**, 31, 2631.
- [82] U. Wiesner, N. Reynolds, C. Boeffel, H. W. Spiess, *Makromol. Chem., Rapid Commun.* **1991**, 12, 457.
- [83] U. Wiesner, N. Reynolds, C. Boeffel, H. W. Spiess, *Liq. Cryst.* **1992**, 11, 251.
- [84] C. Kulinna, S. Hvilsted, C. Hendann, H. W. Siesler, P. S. Ramanujam, *Macromolecules* **1998**, 31, 2141.
- [85] M. Han, M. Kidowaki, K. Ichimura, P. S. Ramanujam, S. Hvilsted, *Macromolecules* **2001**, 34, 4256.
- [86] T. Ubukata, T. Seki, S. Morino, K. Ichimura, *J. Phys. Chem. B* **2000**, 104, 4148.
- [87] C. Ohe, H. Kamijo, M. Arai, M. Adachi, H. Miyazawa, K. Itoh, T. Seki, *J. Phys. Chem. C* **2008**, 112, 172.
- [88] M. Richard-Lacroix, C. Pellerin, *Macromolecules* **2012**, 45, 1946.
- [89] H. Xia, R. Wang, Y. Liu, J. Cheng, G. Zou, Q. Zhang, D. Zhang, P. Wang, H. Ming, R. Badugu, J. R. Lakowicz, *Adv. Opt. Mater.* **2016**, 4, 371.
- [90] Y. Wang, G. Shen, J. Gao, G. Zou, Q. Zhang, *J. Polym. Sci. Part B Polym. Phys.* **2015**, 53, 415.
- [91] C. L. van Oosten, C. W. Bastiaansen, D. J. Broer, *Nature Mater.* **2009**, 8, 677.
- [92] K. M. Lee, M. L. Smith, H. Koerner, N. Tabiryan, R. A. Vaia, T. J. Bunning, T. J. White, *Adv. Funct. Mater.* **2011**, 21, 2913.
- [93] M. Yamada, M. Kondo, R. Miyasato, Y. Naka, J.-i. Mamiya, M. Kinoshita, A. Shishido, Y. Yu, C. J. Barrett, T. Ikeda, *J. Mater. Chem.* **2009**, 19, 60.
- [94] L. A. Nafie, *Appl. Spectrosc.* **1996**, 50, 14A.
- [95] P. J. Stephens, F. J. Devlin, J. J. Pan, *Chirality* **2008**, 20, 643.
- [96] H. Izumi, S. Futamura, L. A. Nafie, R. K. Dukor, *Chem. Rec.* **2003**, 3, 112.
- [97] M. Liu, L. Zhang, T. Wang, *Chem. Rev.* **2015**, 115, 7304.
- [98] G. Iftime, F. Lagugné Labarthe, A. Natansohn, P. Rochon, *J. Am. Chem. Soc.* **2000**, 122, 12646.
- [99] R. M. Tejedor, L. Oriol, J. L. Serrano, F. Partal Ureña, J. J. López González, *Adv. Funct. Mater.* **2007**, 17, 3486.
- [100] J. R. Aviles Moreno, J. J. Lopez Gonzalez, F. Partal Urena, F. Vera, M. B. Ros, T. Sierra, *J. Phys. Chem. B* **2012**, 116, 5090.

- [101] S. R. Domingos, S. J. Roeters, S. Amirjalayer, Z. Yu, S. Hecht, S. Woutersen, *Phys. Chem. Chem. Phys.* **2013**, *15*, 17263.
- [102] A. Ambrosio, L. Marrucci, F. Borbone, A. Roviello, P. Maddalena, *Nat. Commun.* **2012**, *3*, 989.
- [103] L. M. Goldenberg, L. Kulikovskiy, O. Kulikovska, J. Stumpe, *J. Mater. Chem.* **2009**, *19*, 6103.
- [104] J. Vapaavuori, R. H. A. Ras, M. Kaivola, C. G. Bazuin, A. Priimagi, *J. Mater. Chem. C* **2015**, *3*, 11011.
- [105] A. Priimagi, A. Shevchenko, *J. Polym. Sci. Part B Polym. Phys.* **2014**, *52*, 163.
- [106] C. Rianna, M. Ventre, S. Cavalli, M. Radmacher, P. A. Netti, *ACS Appl. Mater. Interfaces* **2015**, *7*, 21503.
- [107] E. Ishow, R. Camacho-Aguilera, J. Guérin, A. Brosseau, K. Nakatani, *Adv. Funct. Mater.* **2009**, *19*, 796.
- [108] R. Kirby, R. G. Sabat, J.-M. Nunzi, O. Lebel, *J. Mater. Chem. C* **2014**, *2*, 841.
- [109] Q. Zhang, X. Wang, C. J. Barrett, C. G. Bazuin, *Chem. Mater.* **2009**, *21*, 3216.
- [110] J. Vapaavuori, V. Valtavirta, T. Alasaarela, J.-I. Mamiya, A. Priimagi, A. Shishido, M. Kaivola, *J. Mater. Chem.* **2011**, *21*, 15437.
- [111] C. Hubert, C. Fiorini-Debuisschert, I. Maurin, J. M. Nunzi, P. Raimond, *Adv. Mater.* **2002**, *14*, 729.
- [112] V. Teboul, R. Barille, P. Tajalli, S. Ahmadi-Kandjani, H. Tajalli, S. Zielinska, E. Ortyl, *Soft Matter* **2015**, *11*, 6444.
- [113] G. Di Florio, E. Brundermann, N. S. Yadavalli, S. Santer, M. Havenith, *Soft Matter* **2014**, *10*, 1544.
- [114] D. Y. Kim, S. K. Tripathy, L. Li, J. Kumar, *Appl. Phys. Lett.* **1995**, *66*, 1166.
- [115] P. Rochon, E. Batalla, A. Natansohn, *Appl. Phys. Lett.* **1995**, *66*, 136.
- [116] S. Ciobotarescu, N. Hurduc, V. Teboul, *Phys. Chem. Chem. Phys.* **2016**, *18*, 14654.
- [117] F. Fabbri, Y. Lassailly, S. Monaco, K. Lahlil, J. P. Boilot, J. Peretti, *Phys. Rev. B* **2012**, *86*.
- [118] N. Hurduc, B. C. Donose, L. Rocha, C. Ibanescu, D. Scutaru, *RSC Adv.* **2016**, *6*, 27087.
- [119] M. Saphiannikova, D. Neher, *J. Phys. Chem. B* **2005**, *109*, 19428.
- [120] M. Saphiannikova, W. Toshchevikov, J. Ilnytskyi, *Nonlinear Optics and Quantum Optics* **2010**, *41*, 27.
- [121] V. Toshchevikov, M. Saphiannikova, G. Heinrich, *J. Phys. Chem. B* **2009**, *113*, 5032.
- [122] N. S. Yadavalli, S. Loebner, T. Papke, E. Sava, N. Hurduc, S. Santer, *Soft Matter* **2016**, *12*, 2593.
- [123] M. L. Juan, J. Plain, R. Bachelot, P. Royer, S. K. Gray, G. P. Wiederrecht, *ACS Nano* **2009**, *3*, 1573.
- [124] P. Lefin, C. Fiorini, J.-M. Nunzi, *Pure Appl. Opt.* **1998**, *7*, 71.
- [125] V. Teboul, M. Saïdine, J. M. Nunzi, J. B. Accary, *J. Chem. Phys.* **2011**, *134*, 114517.
- [126] V. Teboul, *J. Phys. Chem. B* **2015**, *119*, 3854.
- [127] C. Sourisseau, *Chem. Rev.* **2004**, *104*, 3851.
- [128] F. Lagugné Labarthe, T. Buffeteau, C. Sourisseau, *J. Phys. Chem. B* **1998**, *102*, 5754.
- [129] F. Lagugné Labarthe, J.-L. Bruneel, T. Buffeteau, C. Sourisseau, M. R. Huber, S. J. Zilker, T. Bieringer, *Phys. Chem. Chem. Phys.* **2000**, *2*, 5154.
- [130] F. Lagugné Labarthe, J. L. Bruneel, C. Sourisseau, M. R. Huber, V. Börger, H. Menzel, *J. Raman Spectrosc.* **2001**, *32*, 665.
- [131] F. Lagugné Labarthe, T. Buffeteau, C. Sourisseau, *Macromol. Symp.* **1999**, *137*, 75.
- [132] F. Lagugné-Labarthe, C. Sourisseau, R. D. Schaller, R. J. Saykally, P. Rochon, *J. Phys. Chem. B* **2004**, *108*, 17059.
- [133] G. Di Florio, E. Brundermann, N. S. Yadavalli, S. Santer, M. Havenith, *Soft Mater.* **2014**, *12*, S98.

- [134] G. Di Florio, E. Brundermann, N. S. Yadavalli, S. Santer, M. Havenith, *Nano Lett.* **2014**, *14*, 5754.
- [135] T. A. Singleton, K. S. Ramsay, M. M. Barsan, I. S. Butler, C. J. Barrett, *J. Phys. Chem. B* **2012**, *116*, 9860.
- [136] K. E. Snell, N. Stephant, R. B. Pansu, J. F. Audibert, F. Lagugné-Labarthe, E. Ishow, *Langmuir* **2014**, *30*, 2926.
- [137] M. Richard-Lacroix, Y. Zhang, Z. Dong, V. Deckert, *Chem. Soc. Rev.* **2017**, 10.1039/c7cs00203c.
- [138] S. S. Kharintsev, A. I. Fishman, S. K. Saikin, S. G. Kazarian, *Nanoscale* **2016**, *8*, 19867.
- [139] N. Tallarida, L. Rios, V. A. Apkarian, J. Lee, *Nano Lett.* **2015**, *15*, 6386.
- [140] B. C. Galarreta, I. Rugar, A. Young, F. Lagugné-Labarthe, *J. Phys. Chem. C* **2011**, *115*, 15318.
- [141] M. Tabatabaei, A. Sangar, N. Kazemi-Zanjani, P. Torchio, A. Merlen, F. Lagugné-Labarthe, *J. Phys. Chem. C* **2013**, *117*, 14778.
- [142] Z. Zhang, M. Richard-Lacroix, V. K. Deckert, *Faraday Discuss.* **2017**, 10.1039/c7fd00157f.
- [143] J. Vapaavuori, A. Laventure, C. G. Bazuin, O. Lebel, C. Pellerin, *J. Am. Chem. Soc.* **2015**, *137*, 13510.
- [144] J. E. Koskela, J. Vapaavuori, R. H. A. Ras, A. Priimagi, *ACS Macro Lett.* **2014**, *3*, 1196.
- [145] A. Dazzi, C. B. Prater, *Chem. Rev.* **2016**, *117*, 5146.
- [146] E. A. Muller, B. Pollard, M. B. Raschke, *J. Phys. Chem. Lett.* **2015**, *6*, 1275.

### Author bios and photographs:



**JV:** Jaana Vapaavuori defended her doctoral thesis, “The Supramolecular Design of Efficient Photoresponsive Materials”, under the supervision of Dr. Arri Primagi and Prof. Matti Kaivola, in the department of Applied Physics at Aalto University, Helsinki, Finland, in 2013. Currently, she is a Banting Postdoctoral Fellow in the Department of Chemistry at the Université de Montreal, Canada, working together with Profs. Geraldine Bazuin and Christian Pellerin. Her main research interests involve developing new materials and supramolecular design concepts for light-controllable nanostructures and liquid crystals, for all-optical surface patterning of polymers, and for electrochemical devices.



**CGB:** Geraldine Bazuin, who obtained her Ph.D. at McGill University in 1984 on ionomers, followed by a postdoc in Strasbourg, France in the area of liquid crystals, was professor in the Department of Chemistry at Université Laval from 1986 to 2003, and then at the Université de Montréal since 2003. She led one of the pioneering research groups working with supramolecular sidechain liquid crystal polymers, focusing especially on ionic bond systems. In more recent years, her work has included azo-containing small molecules and has embraced supramolecular block copolymer systems, particularly in the form of dip-coated and Langmuir-Blodgett thin films.



**CP:** Christian Pellerin is full professor in the Department of Chemistry at the Université de Montréal since 2016. He received his B.Sc. in chemistry in 1997 from Université du Québec à Trois-Rivières and his Ph.D. in polymer chemistry in 2002 from Université Laval under the supervision of Profs. Michel Pérolet and Robert E. Prud'homme. Following a postdoctoral fellowship with Profs. John F. Rabolt and D. Bruce Chase at the University of Delaware, he joined the faculty at the Université de Montréal in 2005. His research interests include azomaterials, electrospun nanofibers, molecular glasses and supramolecular polymer complexes, in addition to developing novel infrared and Raman spectroscopy techniques.

**The table of contents entry: Vibrational spectroscopy techniques provide molecular insight into the photoresponse of chemically specific molecular moieties and are therefore invaluable tools to understand how the molecular-scale photoisomerization of azobenzenes is translated into photoinduced orientation, chirality, self-assembly and mass transport of macromolecules.**

Jaana Vapaavuori,\* C. Geraldine Bazuin, Christian Pellerin\*

### **Taming macromolecules with light – Lessons learned from vibrational spectroscopy**

ToC figure:

